AD-A164 276 CYLINDRICAL GAUSSIAN EIGENMODES OF A RECTANGULAR WAVEGUIDE RESONATOR THRE..(U) CALIFORNIA UNIV SANTA BARBARA QUANTUM INST A AMIR ET AL. 1984 TR-24 1/1

UNCLASSIFIED N00014-80-C-0308 F/G 20/14 NL

END

FILMED

DTIC

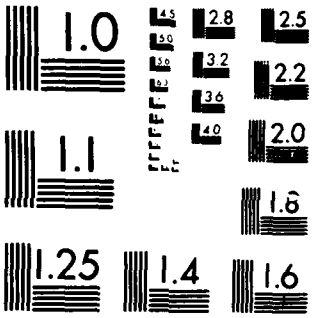


MICROCOPY RESOLUTION TEST CHART

NATIONAL BUREAU OF STANDARDS 1963 A

## REPORT DOCUMENTATION PAGE

READ INSTRUCTIONS BEFORE COMPLETING FORM

| | |
|---|---|
| 1. REPORT NUMBER: No. 24 | 2. GOVT ACCESSION NO. |
| 3. RECIPIENT'S CATALOG NUMBER: (12) | |
| 4. TITLE (and Subtitle): Cylindrical Gaussian Eigenmodes of a Rectangular Waveguide Resonator Three-dimensional Numerical Calculation of Gain per Mode | 5. TYPE OF REPORT & PERIOD COVER: Technical Report 10/01/83 - 09/30/84 |
| | 6. PERFORMING ORG. REPORT NUMBER |
| 7. AUTHOR(s): Avner Amir, Luis Elias and Juan Gallardo | 8. CONTRACT OR GRANT NUMBER(s): N00014-80-C-0308 |
| 9. PERFORMING ORGANIZATION NAME AND ADDRESS: University of California, Quantum Institute, Santa Barbara, CA 93106 | 10. PROGRAM ELEMENT, PROJECT, TAS AREA & WORK UNIT NUMBERS: 61153N; RR011-07-06; NR603-001 |
| 11. CONTROLLING OFFICE NAME AND ADDRESS: ONR, 1030 E. Green St., Pasadena, CA 91106 | 12. REPORT DATE: 1984<br>13. NUMBER OF PAGES |
| 14. MONITORING AGENCY NAME & ADDRESS(if different from Controlling Office) | 15. SECURITY CLASS. (of this report): Unclassified/Unlimited<br>15a. DECLASSIFICATION/DOWNGRADING SCHEDULE |

16. DISTRIBUTION STATEMENT (of this Report)

Approved for public release; distribution.



17. DISTRIBUTION STATEMENT (of the abstract entered in Block 20, if different from Report)

18. SUPPLEMENTARY NOTES

International Society for Optical Engineering, Vol. 137 453, 1984.

19. KEY WORDS (Continue on reverse side if necessary and identify by block number)

Cylindrical, Eigenmodes, Three-dimensional, Calculation

20. ABSTRACT (Continue on reverse side if necessary and identify by block number)

First we present approximate analytical solutions to the wave equation inside an overmoded metallic rectangular waveguide. The cold eigenmodes are expressed in terms of cylindrical Gaussian-Hermite functions times trigonometric functions to insure the boundary conditions. Next, we discuss a numerical three-dimensional calculation for a Free Electron Laser (FEL) amplifier which is based on the Liena Wiechert solution of the Maxwell's equations cast in an integral form. This approach is readily and efficiently extended to include the effects of the metall boundaries of the waveguide by means of the method of "image currents". cont. bac

20.

Finally, the radiation field in the cavity emitted by the electrons in the presence of the combined fields of a co-propagating eigenmode wave plus a linearly polarized magnetic undulator is expanded in terms of cavity eigenmodes. This expansion allows us to compute the gain per resonator mode.

Cylindrical Gaussian Eigenmodes of a
Rectangular Waveguide Resonator
Three-dimensional Numerical Calculation of Gain
per Mode

Avner Amir, Luis Elias, and Juan Gallardo

QIFEL024/83

UNIVERSITY OF CALIFORNIA
SANTA BARBARA
QUANTUM INSTITUTE
FREE ELECTRON LASER PROJECT

# Cylindrical Gaussian Eigenmodes of a Rectangular Waveguide Resonator Three-dimensional Numerical Calculation of Gain per Mode

Avner Amir, Luis Elias, and Juan Gallardo

QIFEL024/83

# Cylindrical Gaussian eigenmodes of a rectangular waveguide resonator Three-dimensional numerical calculation of gain per mode

Avner Amir, Luis Elias and Juan Gallardo

Quantum Institute, University of California at Santa Barbara, Santa Barbara, California 93106

## Abstract

First we present approximate analytical solutions to the wave equation inside an overmoded metallic rectangular waveguide. The cold eigenmodes are expressed in terms of cylindrical Gaussian-Hermite functions times trigonometric functions to insure the boundary conditions. Next, we discuss a numerical three-dimensional calculation for a Free Electron Laser (FEL) amplifier which is based on the Lienard-Wiechert solution of the Maxwell's equations cast in an integral form. This approach is readily and efficiently extended to include the effects of the metallic boundaries of the waveguide by means of the method of "image currents". Finally, the radiation field in the cavity emitted by the electrons in the presence of the combined fields of a co-propagating eigenmode wave plus a linearly polarized magnetic undulator is expanded in terms of cavity eigenmodes. This expansion allows us to compute the gain per resonator mode.

## Introduction

A rather extensive literature on the 3-d FEL theory is presently available. Progress in this area has been occurring in the last two years as a result of efforts of several groups which have carried out numerical as well as semi-analytical calculations.[1,2,3,4]

The main objectives of these calculations are: 1) to incorporate into the theory the finite transverse dimensions of the optical field so to be able to handle the outstanding problem of the filling factor that plagued the more naive 1-d theories 2) to describe the optical quality, i.e., angular distribution, frequency content 3) and lastly to provide secure ground for the optical-resonator design for FEL.

In this paper we focus our attention on the waveguide resonator of the FEL experiment at the University of California Santa Barbara (UCSB). Its mechanical design and main characteristics are discussed in the accompanying paper.[5]

Practical resonators for FEL must contain the following features in addition of providing the containment needed to propagate the electron beam along the undulator: 1) a means to inject and extract the high current relativistic electron beam 2) possibility of allowing relatively large amplitude for the periodic magnetic field (reducing the gap) to insure above-losses small signal gain 3) small beam waist to increase the small-signal gain of the laser 4) low-losses resonator.

Some of these requirements are not easily met by conventional open resonators in the submillimeter region of the spectrum. An appealing alternative is to use waveguide resonators[6] which offer the advantage of small undulator gap and small optical mode area.

In section II.1 we discuss a metallic waveguide resonator[7] which meets the design criteria numbered above. We present analytical approximate solutions of the wave equation with metallic boundary conditions corresponding to low-order, overmoded, rectangular waveguide with infinite aperture cylindrical mirrors. The solutions, eigenmodes of the "cold" resonator are expressed naturally in terms of cylindrical Gaussian-Hermite functions. In the following section II.2 proceeding according to the standard technique of first assuming perfectly conducting walls, we calculate the waveguide losses from the tangential component of the magnetic field at the walls. We show that the $\Pi$-modes propagate along the z-axis with negligible straight-losses in the far-infrared region.

The section III is dedicated to the numerical calculation of the radiation field produced by a relativistic electron beam inside a waveguide, moving in the combined fields of a linearly polarized magnetic undulator and a propagating eigenmode of the cavity.

All 3-d FEL theories published[1,2,3,4] so far assumed open resonators, i.e., the presence of the metallic walls along the interaction region have been ignored. However, to achieve larger undulator magnetic fields it is imperative to reduce the undulator gap and consequently the height of the cavity.

The radiation from a relativistic electron beam wiggling in the interaction region is concentrated along a narrow cone in the axial-direction with an angular aperture $\sim 1/\sqrt{N}$.

When the transverse dimension of the radiation cone is comparable to the height of the resonator channel then additional interferences occur due to the reflections at the walls, increasing the power density at the observation plane.

To account for these reflections, i.e., to satisfy the metallic boundary conditions, we turn to the "image current" approach[8] (rectangular waveguide) which allows an efficient and fast way of computing the field inside the cavity from the radiation of the electron beam in free space.

The 3-d electromagnetic fields produce by an electron beam in an undulator can be considered as the coherent superposition of radiation pulses produced by each individual electron. Each pulse contains the information about velocity and acceleration of the corresponding electron and is analytically represented by the Lienard-Wiechert solutions.[9]

After adding these solutions and extracting the slowly varying amplitude and phase, by means of the standard averaging procedure over many wavelengths of light we cast the total radiation field as an integral over the "electron" time expended inside the undulator. To solve it numerically it is necessary to know the dynamics of the electrons. This is provided by the pendulum equation.[10]

In section III.3 we show how to expand the total radiation field inside the cavity in the Fresnel approximation as a superposition of the "cold" eigenmodes of the resonator.

In the last section III.4 we define the power gain per mode for the UCSB waveguide resonator and we plot the gain curves as function of the resonance parameter for the first three Gaussian transverse modes. We discuss the relative amplitude of the maximum of the gain curve and its position.

## II. Cold eigenmodes of a waveguide resonator

### 1. Analytical approximate solutions of the wave equation with boundary conditions

The UCSB FEL waveguide is a metallic rectangular cross section channel that allows both small undulator gap and small radiation field beam waist. The geometry of the problem is shown in Figure 1 as well as the approximate dimensions of the cavity.

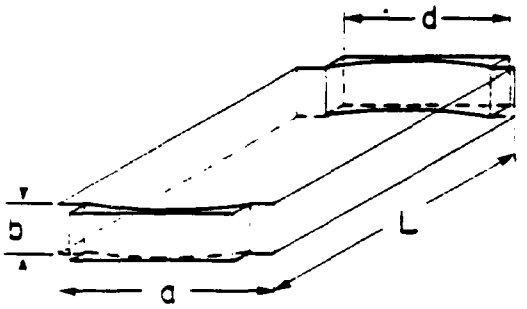


Figure 1. A schematic drawing of the UCSB FEL resonator. a=13.34 cm, b=1.9 cm, d=10.0 cm, L=7.14 cm and the mirror radius of curvature $R_c$=500.0 cm.

First, we find solutions to the wave equation inside a perfect infinitely-long rectangular waveguide in terms of cylindrical waves propagating along the guide axis. Each Cartesian component of the field must satisfy the Helmholtz equation:

$$(\nabla^2+k^2)\ u(x,y,z) = 0 \qquad k = \omega/c \tag{1}$$

where a time dependence $e^{-i\omega t}$ has been assumed.

We are interested in solutions that satisfy the boundary conditions at the vertical parallel planes y=0 and y=b. The proposed solutions are of the functional form:

$$u(x,y,z) = \psi(x,z)e^{i\beta z}\sin\gamma y \qquad \gamma = n\pi/b \quad , \quad \beta = \sqrt{k^2-\gamma^2} \tag{2}$$

where n is an integer 1,2,..... .

Inserting (2) into (1) yields the following equation for the slowly varying complex function $\psi(x,z)$

$$\left(\frac{\partial^2}{\partial x^2} + 2i\beta\frac{\partial}{\partial z} + \frac{\partial^2}{\partial z^2}\right)\psi(x,z) = 0 \tag{3}$$

The slowly varying assumption means that $\frac{1}{\beta}\frac{\partial\psi}{\partial z} \ll 1$, and therefore we can neglect $\frac{\partial^2\psi}{\partial z^2}$ in 3.

Thus, we obtain the standard paraxial differential equation, the solution of which in the context of light beams are well known[11] and can be written as

$$\psi_{mn}(x,z) = \exp(-x^2/w(z)^2 2)\ \exp(i\beta_n x^2/2\ R(z) - (m+1/2)\tan^{-1}(z/z_o))\ H_m(x/w(z))\ N_m \qquad (4)$$

where:

$$N_m = \left( 2^m m! \sqrt{\pi} \sqrt{1+(z/z_o)^2} \right)^{-\frac{1}{2}} \qquad \text{NORMALIZATION CONSTANT}$$

$H_m(x)$ HERMITE POLYNOMIAL

$$w(z) = w_o \sqrt{1 + (z/z_o)^2} \qquad \text{BEAM WAIST} \qquad (5)$$

$$R(z) = z(1 + (z/z_o)^2) \qquad \text{RADIUS OF CURVATURE}$$

$$z_o = \beta w_o^2 \qquad \text{RAYLEIGH LENGTH}$$

If the origin of coordinates is at the minimum spot size.

In practical FEL waveguide resonator designs, the transverse dimensions of the waveguide are usually much larger than the guide wavelength. Consequently, the amplitude of the longitudinal component of the $E_z(x,y,z)$ ($H_z(x,y,z)$) will be much smaller than the corresponding transverse components.[12] The assumption of slow amplitude and phase variations of $\psi(x,z)$ with z in conjunction with the above restriction impose on our theory a limitation to low-order and low-losses modes.

We break down our solutions into two sets of linearly independent functions: a) those for which $E_y$, $E_z \ll E_x$ will be denoted as $\phi^{\tau}_{mn}(x,y,z)$ -modes, i.e., the main cartesian component is parallel to the wide dimension of the guide; b) $H_y$, $H_z \ll H_x$ will be designated as $\phi^{\sigma}_{mn}(x,y,z)$ in this case the dominant electric field cartesian component is perpendicular to the wide dimension of the guide. The boundary condition imposed on the $\tau$-eigenmodes is, $E_x$, $E_z = 0$ at y=0, b for perfect conducting walls; for $\sigma$-eigenmodes the boundary condition is $H_y = 0$ at $y = 0,b$. These are the restrictions at the two parallel horizontal planes; at the vertical planes $x = -a/2, +a/2$ the boundary conditions are automatically satisfied because all field amplitudes drop exponentially as a function of coordinate x (the scale being $w(z)$, the beam waist).

We present below a summary of both type of solutions,

Table I.

| $E^{\tau}_{mn}$-Modes $= \phi^{\tau}_{mn} \exp(i\beta_n z)$ | $E^{\sigma}_{mn}$-Modes $= \phi^{\sigma}_{mn} \exp(i\beta_n z)$ |
|---|---|
| $E_x = \psi_{mn}(x,z)\ \sin(\gamma_n y)\ \exp(i\beta_n z)$ | $E_y = \psi_{mn}(x,z)\ \cos(\gamma_n y)\ \exp(i\beta_n z)$ |
| $E_z = i/\beta_n \frac{\partial \psi_{mn}}{\partial x} \sin(\gamma_n y)\ \exp(i\beta_n z)$ | $E_z = i/\beta_n \frac{\partial E_y}{\partial y}$ |
| $H_y = \beta_n/\omega\mu_o\ E_x$ | $H_x = \beta_n/\omega\mu_o\ E_y$ |
| $H_z = i/\omega\mu_o \frac{\partial E_x}{\partial y}$ | $H_z = -i/\omega\mu_o \frac{\partial \psi_{mn}}{\partial x}\ \cos(\gamma_n y)\ \exp(i\beta_n z)$ |

In Figure 2 we illustrate the configuration of electric field lines at the band waist of various low-order modes.

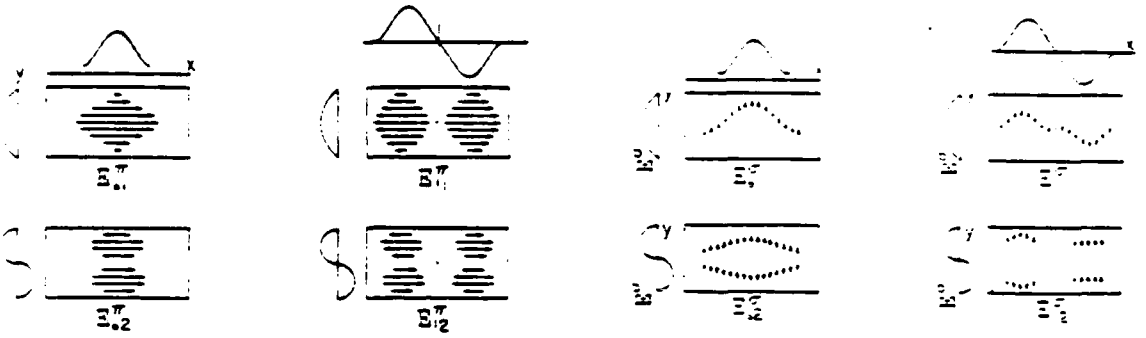

Figure 2. Electric field lines at the waist of low-order waveguide eigenmodes: a) π-modes; b) σ-modes.

For a linearly polarized undulator the appropriate modes that will couple to the electron beam correspond to m=even and n=odd. However, as we shall show in the next subsection, the $\phi^{\sigma}_{02k+1}$ modes have losses that increase with frequency and consequently they are not suitable for FEL operation in the submillimeter region. On the other hand the $\phi^{\pi}_{02k+1}$ modes have a power attenuation constant that decreases with frequency.

## 2. Waveguide losses.

The losses due to the finite conductibility of the walls are computed in the standard fashion by evaluating the tangential component of the magnetic field H at the walls; the results are,

$$\alpha^{\pi}_{mn} = \mu_c \delta / \mu_o b^3 \, (n\pi)^2 \Big/ \sqrt{\mu_o \epsilon_o \omega^2 - n^2\pi^2/b^2} \qquad (6a)$$

$$\alpha^{\sigma}_{mn} = \mu_c \delta / \mu_o b \sqrt{\mu_o \epsilon_o \omega^2 - n^2\pi^2/b^2} \qquad (6b)$$

In Figure 3 we plot the theoretical attenuation constant as given in Eqs. 6 as a function of b, the height of the resonator channel, and we compare them to those of conventional microwave modes in rectangular waveguides. The π-modes losses are two orders of magnitude below those of the more conventional $TE_{01}$-mode for b=20 mm.

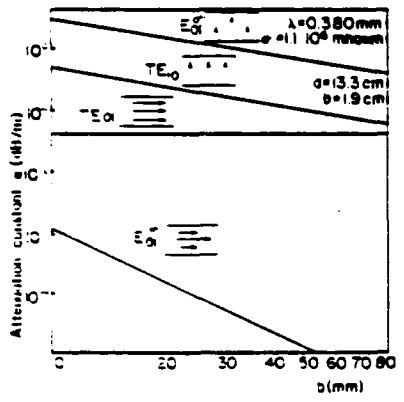


Figure 3. Attenuation constant vs. guide height b.

A description of the actual mechanical design and parameters of the UCSB FEL resonator are discussed in the paper at this conference by one of us (L.E.) and J. Ramian.[5]

## III. Three-dimensional numerical calculation of the FEL radiation

### 1. Slowly varying Lienard-Wiechert solution

The explicit solution of the Maxwell's equations for a point charge in free space can be written as,

$$\vec{E}(\vec{r},t) = e/c \left[ \frac{\vec{n}\Lambda((\vec{n}-\vec{\beta})\Lambda\dot{\vec{\beta}})}{R(1-\vec{\beta}\cdot\vec{n})} \right]_{ret} \qquad (7)$$

these are the Lienard-Wiechert fields, where: e is the electron charge, $\vec{\beta}$, $\dot{\vec{\beta}}$, $R = |r - r'|$ are respectively the instantaneous normalized velocity and acceleration of the particle,

the distance from the position of the particle at time t' to the observation point; and $\vec{n} = \vec{R}/R$. The square bracket has the meaning that the quantity inside it has to be evaluated at the retarded time $t' = t - R(t')/c$.

The total field $\vec{E}(\vec{r},t) = \sum_{i=1}^{N} \vec{E}_i(\vec{r},t)$ is obtained by summing all electrons in the electron beam. It will contain a fast varying factor of the form $e^{i(kz-\omega t)}$ where $\omega \sim 2\gamma^2\omega_o$ (center frequency of the emitted radiation) and $\omega_o = 2\pi c/\lambda_o$ is the frequency corresponding to the period of the wiggler.

To extract the slowly varying (slow) part from $\vec{E}(\vec{r},t)$ we proceed in the usual fashion of multiplying by the fast factor and then averaging over many wavelength of light. This procedure assumes the laser is well above threshold and that nearly coherence and monochromaticity have been achieved.

The fast part of the radiation field can be visualized as produced by electrons in the combined field of an undulator and the optical field $E_x^T(\vec{r},t)$ following the zero order trajectory,

$$\vec{r} = z_o\vec{e}_3 + c\beta_o t'\,\vec{e}_3 - \frac{K}{\gamma}\frac{1}{k_o}\,\sin k_o t'\,\vec{e}_1 \tag{8}$$

where $K = eB_o/mc^2k_o$, $c\beta_o$ is the initial longitudinal velocity, $k_o$ is the undulator wavevector and $\vec{B} = B_o \sin\omega_o t\vec{e}_2$ is the linearly polarized undulator magnetic field. Any departure from zero-order trajectory, due to the ponderomotive potential which force the electrons to bunch and consequently to change their $\beta_z$ velocity, will provide the slow part of the field.

The resulting field after averaging over the total time of interaction $NT = \frac{2\pi}{\omega}N$ (N is the number of periods in the undulator) is,

$$\vec{E}(\vec{r},t) = \left\langle \vec{E}(\vec{r},t) \right\rangle = \frac{ie\omega^2}{2\pi c} \sum^{N_e} \int_0^{NT_o} dt' \,\frac{\vec{n}\Lambda(\vec{n}\Lambda\vec{\beta})}{R}\, e^{i\omega t' + ik(R-z)} \tag{9}$$

where the integral is over the retarded time t' (time of evolution for the electrons), the sum is overall the electrons that at t=0 where inside of a wavelength of light $\lambda$ of the beam ($N_e$); and $T_o$ is the retarded time $T_o = \int_0^T dt/(1-\vec{\beta}\cdot\vec{n})$.

To derive Eq. 9 we assumed electrons pulses $N^{pulse} > NT$ and small signal gain as we maintained the field experienced by the electrons constant over one pass.

To compute this integral we add the single-particle dynamics described by the pendulum equation,[6]

$$\frac{d^2\psi}{d\tau^2} = a(\vec{r})\,\cos(\psi + \phi(\vec{r})) \tag{10}$$

where

$$a(r) = \frac{2\pi eKE_o(\vec{r})LN}{\gamma^2 mc^2}, \qquad \tau = ct'/L$$

$$\psi = \frac{d\psi}{d\tau} \quad \text{and} \quad z(t') = z_o + c\beta_o t' + \delta z.$$

Expanding $R = R_o - n_z\delta z$ and introducing it in Eq. 9 yields,

$$E_x(\vec{r},t) = -\frac{ie\omega^2}{4\pi}\frac{L}{c^2}\frac{K}{\gamma_o}\int_0^{\tau} \frac{e^{-i\psi}}{R_o}\,d\tau \tag{11}$$

where terms proportional to $1/R_o^2$ are neglected; $R_o$ is the distance from the observation point to the zero order position of the particle and we define

$$\psi = n_z k - (1-n_z)\omega t - kR_o - z - z'\,.$$

Equations 10 and 11 completely describe our model[13] and the simultaneous numerical solution of them give the radiation field at the observation point $\vec{r}$ at time t. The geometrical arrangement is in Figure 4.

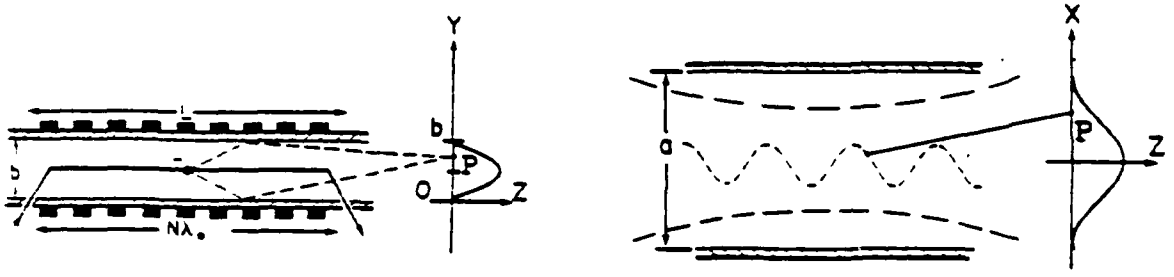


Figure 4. Schematic drawing of a waveguide amplifier. The field at the observation point P is the resultant of superposition of direct wave and reflections from the walls.

## 2. Image current approach.

Our previous discussion assumed no spatial constraints, $E_x(\vec{r},t)$ is the field at any point $\vec{r}$. In the presence of perfect conducting walls the fields must satisfy boundary conditions, i.e., $\vec{E}_{tang} = 0$. When the guide is rectangular an economical method to treat this "real" problem with boundaries is to replace it by another in an enlarger region with "image electron beams" and no boundaries.

Proceeding as in electrostatic, for a waveguide of rectangular cross section we obtain an infinite array of alternating sign currents. The total field at the observation point P is,

$$E_x(\vec{r}) = \sum_{images}^{N_{image}} E_x^k(\vec{r})$$

where $N_{image}$ is the number of image currents that can interfere at that point. The radiation field of each image current is confined to a cone of angle

$$\Delta\theta \sim \sqrt{\theta_p^2 + \frac{0.75}{\gamma^2 N}}$$

where $\theta_p \cong \cos^{-1}(\beta/\beta_{res})$; at a distance z the transverse dimensions of the radiated area is $y_{max} \sim z\Delta\theta$. Hence, the maximum number of images will be

$$N_i \leq y_{max}/b = z/b \sqrt{\theta_p^2 + \frac{0.75}{\gamma^2 N}} \qquad (12)$$

The UCSB FEL resonator has dimensions a=13.34 cm and b=1.9 cm. Using the condition in Eq. 12 we can see that the contribution of image currents with response to the vertical planes are negligible and it is sufficient to include no more than 5 currents in the (y,z) plane, as shown in Figure 5.

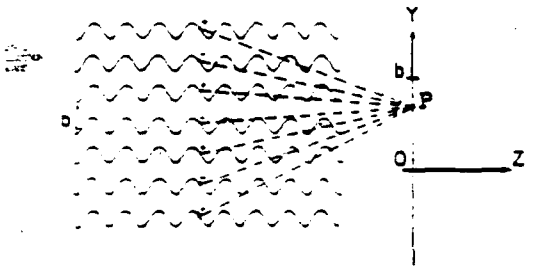


Figure 5. The problem of an electron beam inside a waveguide is replaced by a free-space problem with "image electron beams" which simulate the conducting surfaces.

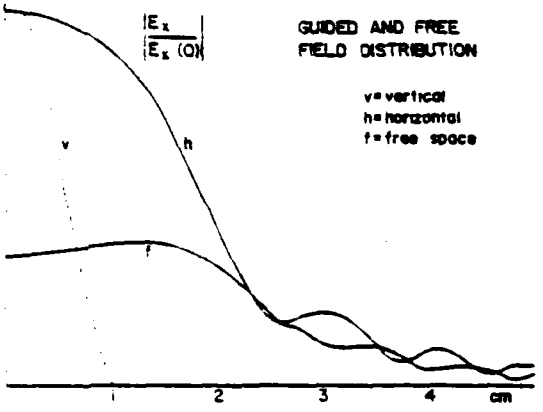


Figure 6. Comparison of the guided radiation field in the x- and y- directions with the free-space case. L=5.7 m and Z=0.78 m.

In Figure 6 we show the angular distribution of the radiation field along both x- and y-axis. For comparison we also plot the free-space distribution. This graph shows the increase of the field on axis respect to the free-space case; the field along the y-axis vanishes beyond x=1.0 cm and the guided field is more concentrated around the z-axis.

## 3. Expansion of radiation field in terms of eigenmodes

If the resonator is designed to operate in one of the transverse eigenmode $\phi_{mn}(x,y,z)$, the presence of the electron beam, i.e., the stimulated radiation produced by it, will tend to create a steady-state with a transverse structure different from the initial one. This state can be expressed as a superposition of transverse eigenmodes of the "cold" resonator,

$$E_x(\vec{r}) = \sum_{mn} A_{mn}\, \phi^{\pi}_{mn}(\vec{r}) \qquad (13)$$

Notice that according to the geometry shown in Figure 4 the electrons will only couple to the $\Pi$-modes; in what follows we will suppress the subscript $\Pi$.

The expansion coefficients $A_{mn}$ can be calculated in a semi-analytical fashion.[13] In Eq. 11 we replace the free-space Green function

$$G_f(\vec{r},\vec{r}') = \frac{e^{ikR}}{R}$$

by the one appropriate to our boundary value problem:

$$G(\vec{r},\vec{r}') = \frac{2\Pi i}{b} \sum_{n=1}^{\infty} H_o^{(1)}(\beta_n \rho)\, \cos\frac{n\Pi}{b}(y-y')$$

where

$$\rho = \sqrt{(x-x')^2 + (z-z')^2}$$

$H_o^{(1)}$ = Hankel function of first kind of order zero.

Subsequently, we use the asymptotic expansion of $H_o^{(1)}$ and after some manipulations we obtain,

$$G(\vec{r},\vec{r}') = \frac{4\pi}{b\omega_o} \sum_{mn} \frac{i^{2m+1}}{\beta_n 2^m m!\sqrt{\pi}}\, \psi_m(x,z)\, \psi_m(x',z')\, \cos\frac{n\pi}{b}(y-y') \qquad (14)$$

where the Fresnel approximation has been used.

Substitution of Eq. 14 into 11 and using completeness yields,

$$A_{mn} = \frac{-i\omega^2 QKL}{c^2 b\omega_o \gamma} \frac{1}{\beta_n} \frac{i^{2m+1}}{2^m m!\sqrt{\pi}} H_m(0) \sum_{i=1}^{N_e} \int_0^{L} e^{-i\psi(z')} \frac{1}{[1+(\frac{z'}{z_0})^2]^{\frac{1}{4}}}\, dz' \qquad (15)$$

where

$$\psi = -\frac{1}{2}(1+2m)\tan^{-1}\frac{z'}{z_0} + n_z\zeta + \tau\frac{\omega L}{c}(1-n_z)\left(1-\beta_0\frac{\omega_0}{\omega}\right)$$

$H_m$ = Hermite polynomial, $n_z = \frac{\beta_n}{\kappa}$ and $Q = I\lambda/(cN_e)$; we have also assumed a filamentary electron beam on axis.

It can be shown that $A_{mn}$ decreases as the Gaussian index m increases.

4. Gain per Mode

We define gain per mode of our single-pass amplifier problem as,

$$G = \frac{\frac{c}{8\pi}\int\left[|\vec{E}_{in}+\vec{E}_{rad}|^2 - |\vec{E}_{in}|^2\right]da}{\frac{c}{8\pi}\int|\vec{E}_{in}|^2da} = 2Re\,\frac{\int\vec{E}_{rad}\,\vec{E}_{in}^{*}da}{\int|\vec{E}_{in}|^2da}$$

where the integral is over the waveguide cross section.

Assuming the incident optical field $E_{in}$ to be the $m^{th}$ eigenmode with amplitude on axis $E_o$ at the beam waist, then

$$G_{mn} = 2Re\,\frac{A_{mn}}{E_o\int da|\phi_{mn}|^2} \qquad (16)$$

m=even; n=odd.

In Figure 7 we plot the gain curve of the three-lowest order Gaussian modes (m=0,2,4) as a function of the resonance parameter $\nu^{1/4}$; the odd-index modes do not couple to the electron beam because they vanish on axis. Similar arguments show that the n index must be odd.

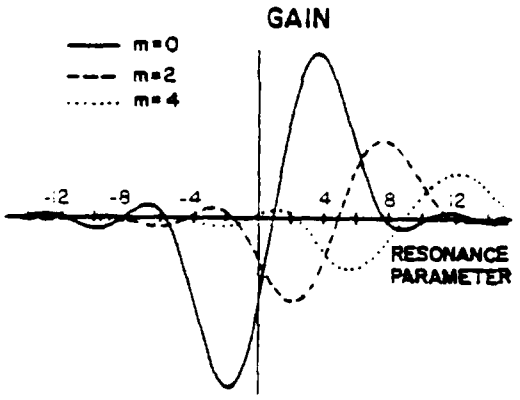


Figure 7. Gain curves for different values of order m=0,2,4 (Gaussian order) with fixed order n=1. Note that maximum value of the gain curve decreases and shifts to a larger resonance parameter.

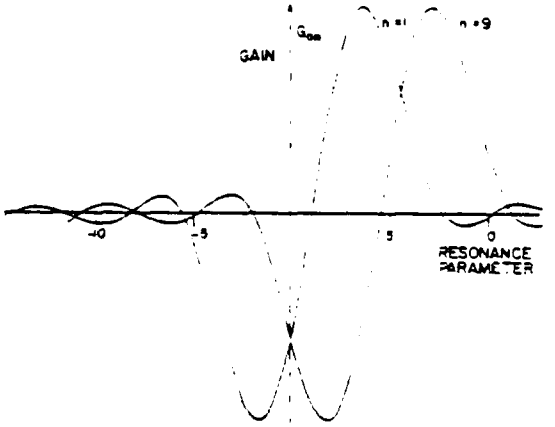


Figure 8. $G_{mn}$ vs. resonance parameter. Gain curves for different values of the order n=1 and 9 (vertical mode) with fixed order m=0. Note the curves are shifted by an amount proportional to $(\beta_n-\beta_{n-1})$ $L(\beta-\beta_{res})$.

Notice the following characteristics: a) The curves are relatively shifted because of the phase shifts associated with each mode. For the parameters (see discussion about Figure 9) of the example shown in Figure 7, the zero of the m=2 mode is underneath the maximum of the m=0 mode. In a mode competition between the two, the m=0 will grow at expense of the m=2. b) The gain of each mode decreases as the m-index increases, as it was indicated at the end of the previous section. Next, in Figure 8 we varied the trigonometric function mode index n.

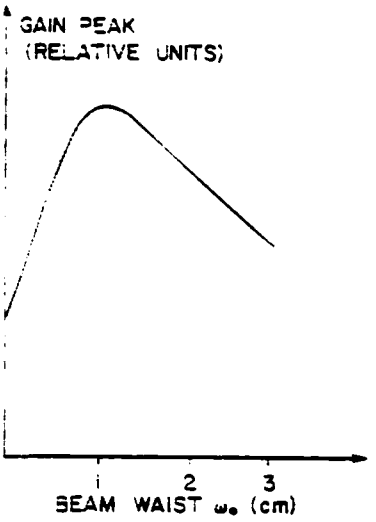


Figure 9. Maximum of gain $G_{mn}$ vs. $\omega_o$ beam waist of input wave. Radiation field is decomposed into eigenmodes $\phi_{mn}(x,y)$ which contain two parameters "beam waist" $\omega_o$ and position of origin of coordinates (i.e., radius of curvature $R(z)$). The best matching of radiation field with input one is obtained with a beam waist $\omega_o$=1.0 cm.

In Figure 9 we plot the value of the maximum gain as a function of the beam waist of the initial optical wave. This result shows that there is an optimal beam waist at about $\omega_o$=1.0 cm; this curve was obtained fixing its position at the center of the undulator.


## Acknowledgement

The authors wish to acknowledge support from the Office of Naval Research and the Air Force Office for Scientific Research under ONR Contract N00014-80-C-308, and helpful discussions with I. Boscolo and W. Colson. We also would like to thank G. Ramian for his work in the mechanical design of the waveguide resonator.


## References


1. Physics of Quantum Electronics Vol. 8 and 9, edited by S. Jacobs, et.al. Addison-Wesley 1982. Chapters 23,26,27,47.
2. Unpublished report, QIFEL015/82 Office of Naval Research Program Review. UCSB Santa Barbara, March 15-16, 1982.
3. Proceedings of the Bendor FEL Conference, Bendor (France) Sept. 26-Oct. 1, 1982.
4. Cha-Mei Tang and P. Sprangle, this volume; P. Elleaume, this volume; J. Slater et.al this volume.
5. L. Elias and G. Ramian, this volume.
6. John Degnan, Appl. Phys. 11, 1 (1976); F. Kneubuhl and E. Affolter, Infrared and Millimeter Waves, Kenneth J. Button editor, vol. 1, 235 (1979).
7. L. Elias and J. Gallardo, Appl. Phys. B31 (1983).
8. Morse and Feshbach, Methods of Theoretical Physics, McGraw-Hill; R.P. Feynman, Lectures on Physics, Vol. II, Chapter 24. Addison-Wesley; R.E. Collin, Field Theory of Guided Waves, McGraw-Hill (1960), p. 34-35.
9. L. Elias and J. Gallardo, Phys. Rev. A24, 3276 (1981).
10. W. Colson, Physics of Quantum Electronics, Vol. 5, edited by S.F. Jacobs et.al, Addison-Wesley, 1975.
11. H. Kogelnik and T. Li, Appl. Opt. 5, 1550 (1966).
12. M. Lax, W. Louisell and W. McKnight, Phys. Rev. A11, 1365 (1975).
13. A. Amir and L. Elias, "Effects of Rectangular Boundaries in Linearly Polarized Wiggler Free Electron Laser" AIAA 16th Fluid and Plasma Dynamics Conference, Boston, MASS; July 12-14, 1983.
14. W. Colson and P. Ellalume, Appl. Phys. B29, 1 (1982).

END

FILMED

3-86

DTIC